Holonomic quantum gates: A semiconductor-based implementation

Holonomic quantum gates: A semiconductor-based implementation

Paolo Solinas,[1] Paolo Zanardi,[2] Nino Zanghì,[1] and Fausto Rossi[2,3]
[1]*Istituto Nazionale di Fisica Nucleare (INFN) and Dipartimento di Fisica, Università di Genova, Via Dodecaneso 33, 16146 Genova, Italy*
[2]*Institute for Scientific Interchange (ISI), Viale Settimio Severo 65, 10133 Torino, Italy*
[3]*Istituto Nazionale per la Fisica della Materia (INFM) and Dipartimento di Fisica, Politecnico di Torino, Corso Duca degli Abruzzi 24, 10129 Torino, Italy*
(Received 20 January 2003; published 27 June 2003)

We propose an implementation of holonomic (geometrical) quantum gates by means of semiconductor nanostructures. Our quantum hardware consists of semiconductor macroatoms driven by sequences of ultrafast laser pulses (*all optical control*). Our logical bits are Coulomb-correlated electron-hole pairs (excitons) in a four-level scheme selectively addressed by laser pulses with different polarization. A universal set of single- and two-qubit gates is generated by adiabatic change of the Rabi frequencies of the lasers and by exploiting the dipole coupling between excitons

DOI: 10.1103/PhysRevA.67.062315 PACS number(s): 03.67.Lx

I. INTRODUCTION

In the recent years, the interest about quantum computation (QC) and quantum information processing (QIP) has been considerably growing. Applications of QIP, e.g., quantum cryptography and quantum teleportation, have been proposed and verified experimentally. In QC, it has been shown that quantum algorithms may speed up some classically intractable problems in computer science [1].

Unfortunately this power inherent to quantum features (i.e., entanglement, state superposition) is difficult to be exploited because quantum states are typically highly unstable, i.e., the undesired coupling with the many degrees of freedom of the environment may lead to decoherence and to the loss of the information encoded. Another source of error can be the imperfect control of parameters driving the evolution of the system. This can lead to wrong output states. To implement effective QIP techniques, these two problems must be faced and solved.

For the problem of decoherence, some methods have been proposed theoretically, for e.g., via error correcting codes [2] it is possible to find errors induced by the environment and correct them. Other approaches propose to encode information in states that are stable against environmental noise [3], or to eliminate dynamically the noise effects ([4,5]). A few quantum hardwares have been proposed for the implementation of quantum gates; e.g., nuclear magnetic resonance [6], ion traps [7–10] semiconductor quantum dots (or macroatoms) ([11–13]); in each of these implementations we have different gates and different ways of processing information.

A conceptually novel approach is *topological computation* ([14,15]) in which the gate parameters depend only on the global features of the control process, being therefore insensitive to the local fluctuations. Though interesting the topological gates proposed so far are quite difficult to realize in practice because they are based on nonlocal quantum states of many-body systems with complex interactions.

Another approach that has some of the global (geometrical) features of the quantum gates and seems closer to the present experimental technology is the the so-called *holonomic quantum computation* (HQC) ([16,17]). In this paper, we shall analyze in a detalied manner a recent proposal for HQC with semiconductor quantum dots [18].

We shall start by recalling the basic facts about HQC (Sec. II) and the excitonic transitions in semiconductor macroatoms (Sec. III). In Sec. IV, we will show how to encode quantum information in excitonic state and how to realize single-qubit gates by means of laser pulses. The two-qubit gates resorting to a biexcitonic shift are illustated in Sec. V. Section VI contains the conclusions, and Appendixes are added to improve the self-consistency of the paper.

II. QUANTUM HOLONOMIES

When a quantum state undergoes an adiabatic cyclic evolution, a nontrivial phase factor appears. This is called *geometrical phase* because it only depends on the global properties, i.e, not on the path in the parameter space but only on the swept solid angle. If the evolving state is nondegenerate, we have only an Abelian phase (Berry phase [19]), but if it is degenerate we have a non-Abelian operator. Then we can use it to process the quantum information encoded in the state.

More precisely, if we have a family $\mathcal{F}$ of isodegenerate Hamiltonians $H(\lambda)$ depending on m dynamically controllable parameters λ, we encode the information in a n-fold degenerate eigenspace $\mathcal{E}$ of a Hamiltonian $H(\lambda_0)$. Changing λ's and driving $H(\lambda)$ along a loop, we produce a nontrivial transformation of the initial state, $|\psi_0\rangle \to U|\psi_0\rangle$.

These transformations, called *holonomies*, are the generalization of Berry's phase, and can be computed in terms of the Wilczek-Zee gauge connection [20]: $U(C) = \mathbf{P}\exp(\oint_C A)$, where P denotes path orderings, C is the loop in the parameter space, and $A = \Sigma_{\mu=1}^{m} = A_\mu d\lambda_\mu$ is the $u(n)$-valued connection. If $|D_i(\lambda)\rangle$ $(i=1,\ldots,n)$ are the instantaneous eigenstates of $H(\lambda)$, the connection is $(A_\mu)_{\alpha\beta} = \langle D_\alpha | \partial/\partial\Omega^\mu | D_\beta \rangle$ $(\alpha,\beta=1,\ldots,n)$.

It is useful to introduce the *curvature* two-form $F = \Sigma_{\mu\nu} F_{\mu\nu} dx^\mu \wedge dx^\nu$, where $F_{\mu\nu} = \partial_\mu A_\nu - \partial_\nu A_\mu + [A_\mu, A_\nu]$; F allows us to evaluate the dimension of the holonomy group and when this coincides with the dimension of $U(n)$ we are

able to perform the universal quantum computation with holonomies.

For computation purposes, we note that if the connection components commute $[A_\mu, A_\nu]=0$, the curvature reduces to $F_{\mu\nu}=\partial_\mu A_\nu - \partial_\nu A_\mu$ and we can use Stokes theorem to compute the holonomies. The holonomic transformation can be calculated easily $U=\exp(i\int_S F_{\mu\nu} d\lambda_\mu \wedge d\lambda_\nu)$, and depends on the "flux" of $F_{\mu\nu}$ through the surface S delimited by C. It is now clear that holonomies are associated to the geometrical features of the parameter space.

Even if with an holonomy we can build every kind of transformation (logical gate), it is useful to think in terms of few simple gates that constitute a universal set (i.e., which can be composed to obtain any unitary operator).

Many efforts have been made to implement geometrical quantum gates (i.e., nuclear magnetic resonance [21] or superconducting nanocircuits [22]) because they are believed to be fault tolerant for errors due to an imperfect control of parameters [23,24]. The nonadiabatic realizations of Berry's phase logic gates have been studied as well [25–28]. More recently, schemes for the experimental implementation of non-Abelian holonomic gates have been proposed for atomic physics, [29] ion traps [30], Josephson junctions [31], Bose-Einstein condensates [32], and neutral atoms in cavity [33].

The basic idea is to have a four-level Λ system with an excited state ($|e\rangle$) connected to a triple degenerate space with the logical qubits ($|0\rangle$ and $|1\rangle$) and an *ancilla* qubit ($|a\rangle$); the three degenerate states are separately addressed and controlled. The effective interaction Hamiltonian describing the system is (in interaction picture)

$$H_{int}=\hbar|e\rangle(\Omega_0\langle 0|+\Omega_1\langle 1|+\Omega_a\langle a|)+\text{H.c.} \qquad (1)$$

H possesses a two degenerate states (called *dark states*) with $E(t)=0$ and two *bright states* with $E(t)=\pm\Omega$ ($\Omega=\sqrt{|\Omega_0|^2+|\Omega_1|^2+|\Omega_a|^2}$). At $t=0$, we codify the logical information in one of these dark states (i.e., $|0\rangle$ or $|1\rangle$) and then, changing the Rabi frequencies (Ω_i, $i=0$, 1, a), we perform a loop in the parameter space $[H(0)=H(T)]$. If the adiabatic condition is fullfilled at a generic time t, the state of the system will be a dark state of $H(t)$ and the Hamiltonian loop will correspond to a loop for the state vector. Since for the adiabatic condition the excited state is never populated, the instantaneous dark state will be a superposition of the degenerate states. With this loop, we produce a rotation in the degenerate space ($|0\rangle$, $|1\rangle$, $|a\rangle$), starting from a logical qubit and passing through the *ancilla* qubit. At the beginning and at the end of the cycle, we have only logical bits, but after a loop a geometrical operator is applied to them. Since we can diagonalize (1), it is easy to calculate the connection and the holonomy associated to the loop.

We can construct two single-qubit gates: $U_1=e^{i\phi_1|1\rangle\langle 1|}$ (*selective phase shift*) and $U_2=e^{i\phi_2\sigma_y}$ $[\sigma_y=i(|1\rangle\langle 0|-|0\rangle\langle 1|)]$. These two gates ($U_1$ and U_2) are noncommutable, so we can construct non-Abelian holonomies since $U_1U_2\neq U_2U_1$.

To obtain a universal set of gates, we must introduce a two-qubit gate; since these gates exploit the interaction between two qubits, they will depend on the physical systems considered. A common choice ([18,30]) is to realize a selective phase shift gate $U_3=e^{i\phi_3|11\rangle\langle 11|}$.

TABLE I. Γ_6 (conduction band), Γ_7, Γ_8 periodic part of Bloch function.

$\lvert J_{tot}, J_z\rangle$	Ψ	Γ
$\lvert\frac{1}{2},\frac{1}{2}\rangle$	$i\lvert S\uparrow\rangle$	Γ_6
$\lvert\frac{1}{2},-\frac{1}{2}\rangle$	$i\lvert S\downarrow\rangle$	Γ_6
$\lvert\frac{3}{2},\frac{3}{2}\rangle$	$\frac{1}{\sqrt{2}}\lvert(X+iY)\uparrow\rangle$	Γ_8 (HH)
$\lvert\frac{3}{2},-\frac{3}{2}\rangle$	$\frac{1}{\sqrt{2}}\lvert(X-iY)\downarrow\rangle$	Γ_8 (HH)
$\lvert\frac{3}{2},\frac{1}{2}\rangle$	$-\sqrt{\frac{2}{3}}\lvert Z\uparrow\rangle+\frac{1}{\sqrt{6}}\lvert(X+iY)\downarrow\rangle$	Γ_8 (LH)
$\lvert\frac{3}{2},-\frac{1}{2}\rangle$	$-\sqrt{\frac{2}{3}}\lvert Z\downarrow\rangle-\frac{1}{\sqrt{6}}\lvert(X-iY)\uparrow\rangle$	Γ_8 (LH)
$\lvert\frac{1}{2},\frac{1}{2}\rangle$	$\frac{1}{\sqrt{3}}\lvert Z\uparrow\rangle+\frac{1}{\sqrt{3}}\lvert(X+iY)\downarrow\rangle$	Γ_7
$\lvert\frac{1}{2},-\frac{1}{2}\rangle$	$\frac{1}{\sqrt{3}}\lvert Z\downarrow\rangle+\frac{1}{\sqrt{3}}\lvert(X-iY)\uparrow\rangle$	Γ_7

III. EXCITONIC TRANSITIONS

In what follows, we show that if we can act on a quantum dot with coherent optical (laser) pulses, we can produce Coulomb-correlated electron-hole pairs (excitons) and deal with an interaction Hamiltonian similar to the one described in Eq. (1). By changing the laser parameters along the adiabatic loop, we can produce the same single-qubit gates as in Ref. [30].

In the GaAs-based III-V compounds, the six electrons in the valence band are divided in a quadruplet (Γ_8 symmetry) which corresponds to $J_{tot}=3/2$, and a doublet (Γ_7 symmetry) which corresponds to $J_{tot}=1/2$. If we consider a $GaAs/Al_xGa_{1-x}As$ quantum dot, the confining potential (along the z growth axis) breaks the symmetry and lifts the degeneracy [34]. The states of the quadruplet are separated in $J_z=\pm 3/2$ [*heavy holes* (HH)] and $J_z=\pm 1/2$ [*light holes* (LH)]. The Γ_7 electrons have $J_z=\pm 1/2$. We can rewrite the eigenstates of J_{tot} and J_z using the $|S\rangle$, $|X\rangle$, $|Y\rangle$, $|Z\rangle$ states (the four Γ point Bloch function, Table I).

If we shine the quantum dot with a laser beam, we excite an electron from the valence band to the conduction band. In the dipole approximation, we have to calculate the amplitude transition $\langle f|\boldsymbol{\epsilon}\cdot\mathbf{r}|i\rangle$ (where $\boldsymbol{\epsilon}$ is the polarization vector of the electromagnetic wave, $|i\rangle$ and $|f\rangle$ are the initial and final states respectively).

The only nonvanishing transition amplitudes for our calculations are $\langle S|x|X\rangle$, $\langle S|y|Y\rangle$, $\langle S|z|Z\rangle$.

Using this relation and Table I, we can calculate which transitions are allowed and which ones are forbidden.

First we note that, for states such as $|(X+iY)\rangle$, we can

have a transition only using the ''negative'' circularly polarized light, $\boldsymbol{\epsilon}=\boldsymbol{\epsilon}_x-i\boldsymbol{\epsilon}_y$,

$$\begin{aligned}\langle S|\boldsymbol{\epsilon}\cdot\mathbf{r}|(X+iY)\rangle&=\langle S|(x-iy)|(X+iY)\rangle\\&=\langle S|x|X\rangle+\langle S|y|Y\rangle\\&=2\langle S|x|X\rangle\end{aligned}\tag{2}$$

($\langle S|x|X\rangle=\langle S|y|Y\rangle$ for the symmetry of our system).

Using ''positive'' circularly polarized light, we have no transition,

$$\begin{aligned}\langle S|\boldsymbol{\epsilon}\cdot\mathbf{r}|(X+iY)\rangle&=\langle S|(x+iy)|(X+iY)\rangle\\&=\langle S|x|X\rangle-\langle S|y|Y\rangle\\&=0.\end{aligned}\tag{3}$$

The latter are called *polarization selection rules* (PSR).

We have also to consider the spin wave function in the initial and final states. If the initial state has spin up (down) the final state must have spin up (down) [*spin selection rules* (SSR)]. For example,

$$\langle S|(x-iy)|(X+iY)\rangle\langle\uparrow|\uparrow\rangle=2\langle S|x|X\rangle,$$

$$\langle S|(x-iy)|(X+iY)\rangle\langle\uparrow|\downarrow\rangle=0.\tag{4}$$

A. Heavy-hole transitions

From Table I, we have the heavy hole and the Γ_6 (conduction band) states; using SSR we can say that the only allowed transitions are

$$\left|\frac{3}{2},\frac{3}{2}\right\rangle=\frac{1}{\sqrt{2}}|(X+iY)\uparrow\rangle\rightarrow\left|\frac{1}{2},\frac{1}{2}\right\rangle=i|S\uparrow\rangle,$$

$$\left|\frac{3}{2},-\frac{3}{2}\right\rangle=\frac{1}{\sqrt{2}}|(X-iY)\downarrow\rangle\rightarrow\left|\frac{1}{2},-\frac{1}{2}\right\rangle=i|S\downarrow\rangle.$$

The first transition is produced by the ''negative'' circularly polarized light (we write the corresponding operator as σ^-) and the second transition is produced by the ''positive'' circularly polarized light (σ^+) for the PSR.

In terms of excitons (electron-hole pairs), if we perform a transition with σ^-, we promote an electron with spin 3/2 of the valence band to the conduction band with spin 1/2, and we get an exciton with angular momentum -1 (E^-). With σ^+ we promote an electron with spin $-3/2$ of the valence band to the conduction band with spin 1/2, and we have an exciton with angular momentum 1 (E^+).

B. Light-hole transitions

For the light hole, we have more allowed transitions; this is due to the presence of the $|Z\rangle$ states in the wave function. As for the HH transitions, using $\sigma^\pm$ we have

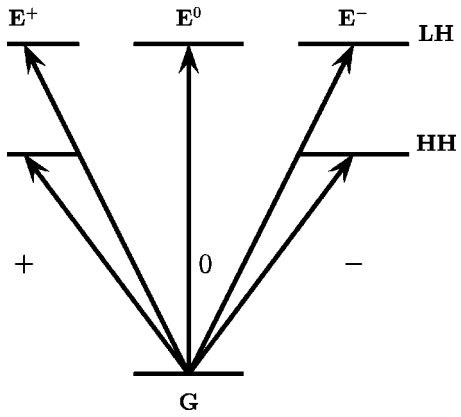

FIG. 1. Level scheme for LH and HH.

$$\left|\frac{3}{2},\frac{1}{2}\right\rangle\rightarrow\left|\frac{1}{2},-\frac{1}{2}\right\rangle\quad\text{for}\quad\sigma^-,$$

$$\left|\frac{3}{2},-\frac{1}{2}\right\rangle\rightarrow\left|\frac{1}{2},\frac{1}{2}\right\rangle\quad\text{for}\quad\sigma^+.$$

These transitions are allowed with circular (positive or negative) polarization ($\boldsymbol{\epsilon}=\boldsymbol{\epsilon}_x\pm i\boldsymbol{\epsilon}_y$) and propagation along the z (growth) axis. If we have the wave propagating along the x or y axis and the polarization along z, then the transition is allowed by PSR. Using also the SSR, we get the two allowed transitions:

$$\left\langle\frac{1}{2},\frac{1}{2}\right|z\left|\frac{3}{2},\frac{1}{2}\right\rangle\sim\langle S|z|Z\rangle,\tag{5}$$

$$\left\langle\frac{1}{2},-\frac{1}{2}\right|z\left|\frac{3}{2},-\frac{1}{2}\right\rangle\sim\langle S|z|Z\rangle.\tag{6}$$

With the operator σ^0, we have the following transitions:

$$\left|\frac{3}{2},\frac{1}{2}\right\rangle\rightarrow\left|\frac{1}{2},\frac{1}{2}\right\rangle\quad\text{for }\sigma^0,$$

$$\left|\frac{3}{2},-\frac{1}{2}\right\rangle\rightarrow\left|\frac{1}{2},-\frac{1}{2}\right\rangle\quad\text{for }\sigma^0.$$

Such transitions with polarization along the z axis have been experimentally observed [35].

Exciting light-hole electrons with three different kinds of light (left and right circular polarization and polarization along z axis), we can induce three different kinds of transitions with the same energy [35].

In terms of excitons if we make a transition with $\sigma^\pm$, we promote an electron with spin $\mp 1/2$ from the valence band to the conduction band with spin $\pm 1/2$, and we get an exciton with angular momentum ± 1 ($E^\pm$). Using light propagating along x or y axis with z polarization, we promote an electron with spin $\pm 1/2$ from the valence band to the conduction band with spin $\pm 1/2$, and we have an exciton with angular momentum 0 (E^0).

The allowed transitions and the corresponding energy-level scheme for HH and LH are shown in Fig. 1.

C. Γ_7 transitions

In the same way we can compute the transition selection rules for the Γ_7 electrons:

$$\left|\frac{1}{2},\frac{1}{2}\right\rangle \rightarrow \left|\frac{1}{2},-\frac{1}{2}\right\rangle \quad \text{for } \sigma^-,$$

$$\left|\frac{1}{2},-\frac{1}{2}\right\rangle \rightarrow \left|\frac{1}{2},\frac{1}{2}\right\rangle \quad \text{for } \sigma^+,$$

$$\left|\frac{1}{2},\frac{1}{2}\right\rangle \rightarrow \left|\frac{1}{2},\frac{1}{2}\right\rangle \quad \text{for } \sigma^0,$$

$$\left|\frac{1}{2},-\frac{1}{2}\right\rangle \rightarrow \left|\frac{1}{2},-\frac{1}{2}\right\rangle \quad \text{for } \sigma^0.$$

Like for the LH, we have three different kinds of transitions that can be distinguished by the light polarization.

Those transitions are energetically higher with respect to the LH and HH ones. Therefore, we should be able to forbid them using properly tuned laser sources with bandwidth $\Delta E < E_{\Gamma_7} - E_{LH} \simeq 0.3$ eV [36].

IV. EXCITON INTERACTION HAMILTONIAN AND SINGLE-QUBIT GATES

Now we want to write the interaction Hamiltonian for the exciton transitions (excluding Γ_7 transitions).

The Hamiltonian for the light-matter interaction is (we use the electric field instead of the vector potential [37])

$$H_{int} = -e[\vec{P}\cdot\vec{E}^*(t) + \text{H.c.}], \tag{7}$$

where $\vec{E}(t)$ is the electric field, $\vec{P}$ is the polarization operator defined as

$$\vec{P} = \sum_{n,m} v_m^\dagger c_n \langle v,m|e\vec{r}|c,n\rangle = \sum_{n,m} v_m^\dagger c_n \vec{\mu}_{nm}^* \tag{8}$$

and

$$\vec{\mu}_{nm} = \langle c,n|e\vec{r}|v,m\rangle. \tag{9}$$

c_n and $c_n^\dagger$ are the annihilation and creation operators for an electron in the conduction band with spin n ($n=\pm 1/2$); v_m and $v_m^\dagger$ are the annihilation and creation operators for an electron in the valence band with spin m [$m=\pm 1/2$ (LH) or $m=\pm 3/2$ (HH)].

Then, using the dipole approximation [$\vec{E}^*(t) = E_0 e^{i(\mathbf{kx}-\omega t)}\boldsymbol{\epsilon} \approx E_0 e^{-i\omega t}\boldsymbol{\epsilon}$],

$$H_{int} = -\left[\sum_{n,m} v_m^\dagger c_n \langle v,m|e\vec{r}|c,n\rangle \cdot \vec{E}^*(t) + \text{H.c.}\right]. \tag{10}$$

We define

TABLE II. Rabi frequencies for allowed transitions.

$\Omega_{n,m}$	v		c	Exciton
$\Omega_{\frac{1}{2},\frac{3}{2}}$	$\frac{3}{2}$	$\rightarrow$	$\frac{1}{2}$	E^-
$\Omega_{-\frac{1}{2},-\frac{3}{2}}$	$-\frac{3}{2}$	$\rightarrow$	$-\frac{1}{2}$	E^+
$\Omega_{\frac{1}{2},-\frac{1}{2}}$	$-\frac{1}{2}$	$\rightarrow$	$\frac{1}{2}$	E^+
$\Omega_{-\frac{1}{2},\frac{1}{2}}$	$\frac{1}{2}$	$\rightarrow$	$-\frac{1}{2}$	E^-
$\Omega_{\frac{1}{2},\frac{1}{2}}$	$\frac{1}{2}$	$\rightarrow$	$\frac{1}{2}$	E^0
$\Omega_{-\frac{1}{2},-\frac{1}{2}}$	$-\frac{1}{2}$	$\rightarrow$	$-\frac{1}{2}$	E^0

$$\hbar\Omega_{n,m} = \vec{\mu}_{nm}^*\cdot\vec{E}^*(t) = E_0 e^{-i\omega t}\boldsymbol{\epsilon}\cdot\langle v,m|e\vec{r}|c,n\rangle. \tag{11}$$

The last term is the dipole transition amplitude.

The term $c^\dagger_{\pm 1/2} v_{\pm 3/2}$ describes the promotion of an electron with spin $\pm 3/2$ to the conduction band with spin $\pm 1/2$, and then it describes the creation of a ''heavy'' exciton with angular momentum ± 1 ($E^\pm$) from the ground state G. In the same way, we can rewrite the terms in Eq. (10) taking account of the *light-hole* transition. With this new notation, we have nonvanishing coefficients (as discussed in Sec. III) in Table II.

The Hamiltonian becomes

$$H_{int} = -\hbar[\Omega_{-,\text{HH}}|E_H^-\rangle\langle G| + \Omega_{+,\text{HH}}|E_H^+\rangle\langle G| + \Omega_{+,\text{LH}}|E_L^+\rangle \times\langle G| + \Omega_{-,\text{LH}}|E_L^-\rangle\langle G| + \Omega_{0,\text{LH}}|E_L^0\rangle\langle G| + \text{H.c.}]. \tag{12}$$

In the last term, we include the two identical kinds of E^0 excitons.

As we stated before, if we can address the light or heavy hole we can distinguish between $E^\pm_{\text{HH}}$ and $E^\pm_{\text{LH}}$; so using light with specified frequency tuned to LH transition, we can write

$$H_{int} = -\hbar(\Omega_{+,\text{LH}}|E_L^+\rangle + \Omega_{-,\text{LH}}|E_L^-\rangle + \Omega_{0,\text{LH}}|E_L^0\rangle) \times\langle G| + \text{H.c.} \tag{13}$$

This Hamiltonian has the same structure as the one proposed in Ref. [30] to implement the holonomic quantum computation with trapped ions. So we can construct the same geometrical single-qubit gates (U_1 and U_2) using , for example, E^+ and E^- as $|1\rangle$ and $|0\rangle$ bits, respectively, and E^0 as ancilla bit $|a\rangle$.

For the first gate, we choose $\Omega_- = 0$, $\Omega_+ = -\Omega\sin(\theta/2)\, e^{i\varphi}$, and $\Omega_0 = \Omega\cos(\theta/2)$. The dark states are given by $|E^-\rangle$ and $|\psi\rangle = \cos(\theta/2)|E^+\rangle + \sin(\theta/2)e^{i\varphi}|E^0\rangle$. By evaluating the connection associated with this two-dimensional (2D) degenerate eigenspace, it is not difficult to see that the unitary transformation $U_1 = e^{i\phi_1|E^+\rangle\langle E^+|}$ ($\phi_1 = \frac{1}{2}\oint \sin\theta d\theta d\varphi$) can be realized as a holonomy. For the second gate, we choose $\Omega_- = \Omega\sin\theta\cos\varphi$, $\Omega_+ = \Omega\sin\theta\sin\varphi$, and $\Omega_0 = \Omega\cos\theta$. The dark states are now given by $|\psi_1\rangle = \cos\theta\cos\varphi|E^-\rangle + \cos\theta\sin\varphi|E^+\rangle - \sin\theta|E^0\rangle$ and $|\psi_2\rangle = \cos\varphi|E^+\rangle - \sin\varphi|E^-\rangle$. In this case, the unitary transformation $U_2 = e^{i\phi_2\sigma_y}$ (where $\phi_2 = \oint \sin\theta d\theta d\varphi$ and $i\sigma_y = |E^+\rangle\langle E^-| - |E^-\rangle\langle E^+|$) can be implemented.

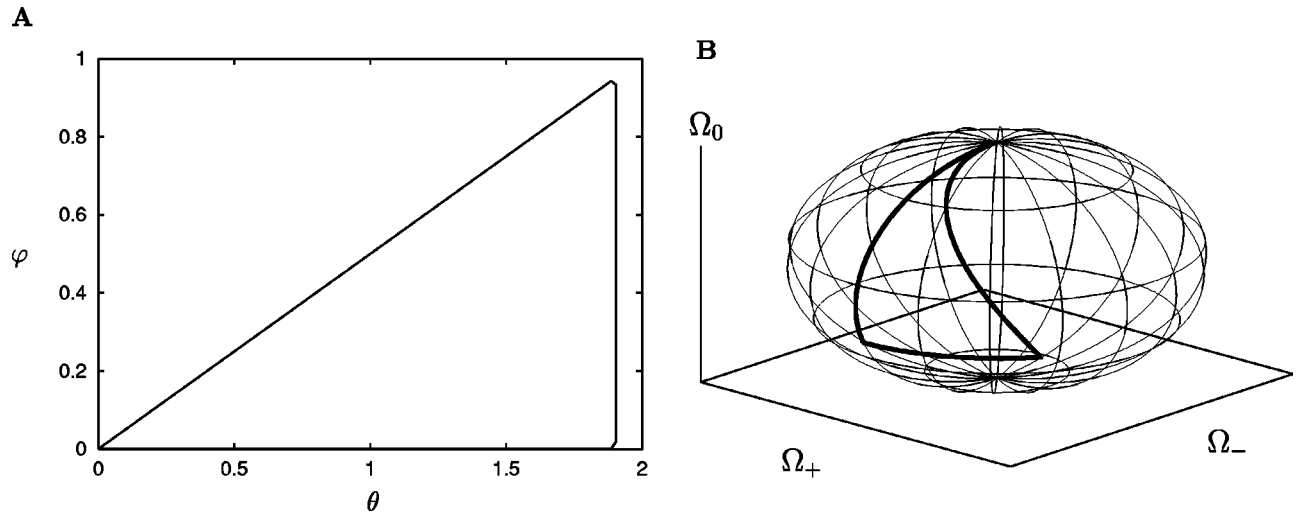

FIG. 2. (a) Loop in the θ-ϕ parameter space. (b) Evolution of $|E^+\rangle$ in the $|E^-\rangle - |E^+\rangle - |E^0\rangle$ space for gate 2 and $\phi_2 = \pi/4$.

We performed numerical simulations to show how our scheme works and how we can satisfy adiabaticity request and apply logical gates. The exciton states have energies between 1.5 eV and 1.7 eV, which correspond to subfemtosecond time scale; then by using femtosecond laser pulse, we avoid transition between the *ground* and exciton states during the evolution. Using Rabi frequencies of about 0.02 fs^{-1} (corresponding to $\Omega^{-1} = 50$ fs) and evolution times of $T_{ad} = 7.5$ ps (as in the simulation), we get for the adiabatic condition $\Omega T_{ad} = 150 \gg 1$, which assures us that there will be no transition between the *dark* and *bright* states (separated by Ω energy).

In Fig. 2(a), the loop in the θ-ϕ space is shown. Since the holonomic operator depends on the solid angle ($\oint d\Omega = \oint d\theta\, d\phi \sin\theta$), the only contribution from this loop comes from the first part and can be easily calculated $\int d\Omega = 1/2(\sin\theta_m - \theta_m \cos\theta_m)$. Then it is sufficient to change θ_m to apply a different operator. In Fig. 2(b), we show the loop in the manifold of the control parameters for gate 2 (Ω^-, Ω^+, Ω^0), since the parameters are real, the 3D vector $\vec{\Omega}$ evolves on a sphere. These two figures refer to the implementation of Hadamard gate [also shown in Figs. 3(b) and (4)], and we choose θ_m in order to obtain $\oint d\Omega = \pi/4$.

Figure 3 shows the state populations during the quantum-mechanical evolution; as we can see, state $|G\rangle$ is never populated (as expected in the adiabatic limit). For the case of gate 1 [see Fig. 3(a)], state $|E^-\rangle$ is decoupled in the evolution while state $|E^+\rangle$ evolves to the ancilla state ($|E^0\rangle$) to eventually end in $|E^+\rangle$ (as we expect for the dark state). In the inset, we show the phase accumulated by $|E^+\rangle$ state; of course, in the central region the phase is undefined.

The quantum evolution of gate 2 in Fig. 3(b) is more complicated because there are no decoupled states, and all the three degenerate states are populated. We start from $|E^+\rangle$ and end in a superposition of $|E^+\rangle$-$|E^-\rangle$. It can be better understood by looking at Fig. 4, where we show the evolution of the dark state in the $|E^+\rangle$, $|E^-\rangle$, $|E^0\rangle$ space. As mentioned above, the initial dark state evolves in the degenerate space: it starts from the $|E^+\rangle$ axis, then passes through a superposition of the three states, and ends in the $|E^+\rangle$-$|E^-\rangle$ plane [$(|E^+\rangle + |E^-\rangle)/\sqrt{2}$ state].

The numerical simulations show that our scheme works, and we are able to produce the desidered gates with realistic

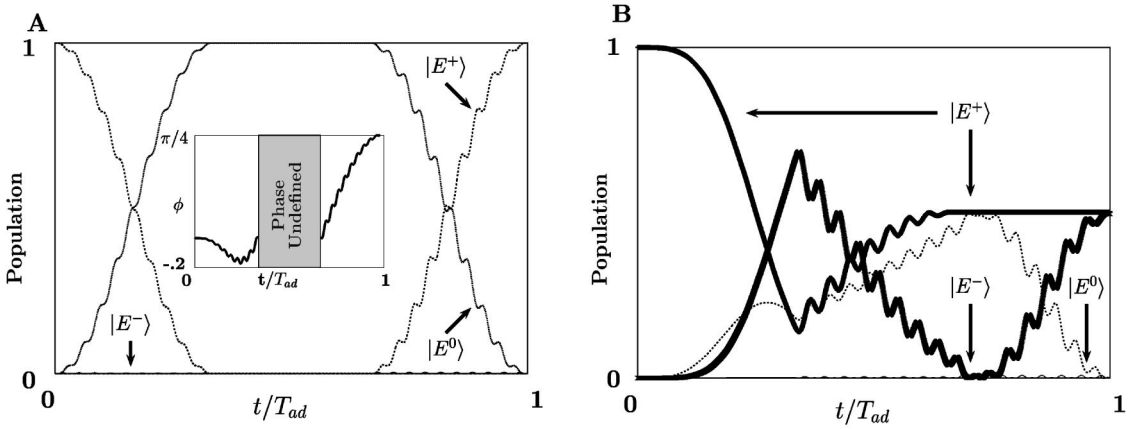

FIG. 3. (a) Simulated time evolution of the HQC gate 1 with $\phi_1 = \pi/4$ and initial state $|E^+\rangle$. The inset shows (where it is defined) the quantity φ, where $\varphi := \arg\langle\Psi(t)|E^+\rangle / |\langle\Psi(t)|E^+\rangle|$. (b) Simulated time evolution of the HQC gate 2 with $\phi_2 = \pi/4$ (Hadamard gate) and initial state $|E^+\rangle$.

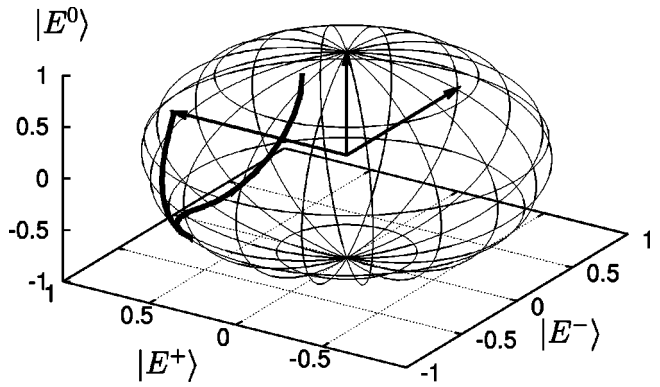

FIG. 4. Evolution of the initial state $|E^+\rangle$ in the $|E^-\rangle - |E^+\rangle - |E^0\rangle$ space for gate 2 and $\phi_2 = \pi/4$.

parameters for the semiconductor quantum dots [38] and for the recent ultrafast laser technology [39]. Moreover, it is clear (also with the gates in Ref. [18]) that we are able to apply different gates in the same gating time because the latter depends only on the adiabatic constraint (and not on the gate we choose) and, through the adiabatic limitation, we can apply several quantum gates. In fact, recent studies [40] have shown that excitons can exhibit a long dephasing time (comparable to hole-electron recombination time) on a nanosecond time scale. The degeneracy in our model has an important role (even if the request can be made weaker and we can use almost-degenerate state i.e. see Sec. IV A), and this can further prolong the dechoerence time till the recombination of light hole.

We are now in a position to make a comparison between the performance of holonomic and standard dynamical quantum gates. From a theoretical point of view, we can apply about 100 single-qubit holonomic gates within decoherence-recombination time. The dynamical gates are faster then the holonomic ones. The gating time depends on the Rabi frequency and the gate we choose, with the parameters used in the previous simulations, we can estimate this operation time to be about 0.1 ps (see e.g., Ref. [13]). In this kind of nanostructures, we have to deal with decoherence times of the order of 100 ps [40], and then one should be able to apply up to thousands of dynamical quantum gates. The comparison gets even worse when one turns to consider two-qubit gate. The dynamical gates can be still realized on the picosecond time scale, whereas the HQC requires much longer time (see e.g., Fig. 7) due to the combination of two concurrent slowing constraints: (1) validity—in the present *particular* HQC scheme—of the second-order perturbative Hamiltonian (14); (2) the adiabaticity requirement with respect to the effective H_{int}.

On the other hand, for the adiabatic model we have just to satisfy the adiabatic condition, that is the choice of the gate applied depends only on the loop in the parameter space; even relatively complicated quantum computations can be enacted by a *single* adiabatic loop. This could open new perspectives in quantum circuits implementation. We can imagine to build quantum algorithms using new fundamental gates that can be applied within the same adiabatic time. Now the task is to find a loop to implement the desired gate, this has been recently studied [41] by numerical simulations; moreover, given a gate we can also find the best loop optimizing the length in the parameter space or satisfying some experimental constraint. It is difficult to apply the same approach to dynamical gates since they are typically thought and performed by sequences of specified building-block operations (e.g., laser-pulse sequences).

For complicated enough operations, one typically needs a lot of dynamical gates; the holonomic approach could be preferred to the dynamical one for its simplicity, i.e., single (few) adiabatic loop versus many dynamical gates, which in turn might even lead to a *shorter* realization time.

A. Laser bandwidth

We saw that by using light with different polarizations, we can induce different transitions and generate $E^{\pm}$, E^0 excitons. To select which electron to excite (HH, LH, Γ_7) we have to use different energies; in fact Γ_7 transitions are the most energetic ones, then there are the LH and the HH transitions.

For circular ($\pm$) polarization light propagating along the z axis, we have [36] the ratios of probabilities to excite the relative electron:

$$\frac{\mathrm{P(HH)}}{\mathrm{P(LH)}} = 3,$$

$$\frac{\mathrm{P(HH)}}{\Gamma_7} = \frac{3}{2}.$$

So it is sufficient that the laser bandwidth is not too large ($\Delta E < E_{\mathrm{LH}} - E_{\mathrm{HH}}$, but $\Delta E \ll E_{\Gamma_7} - E_{\mathrm{LH}}$) to excite HH instead of LH and forbid the Γ_7 transitions.

For light propagating along the $x(y)$ axis with z polarization, the HH transitions are forbidden and

$$\frac{\mathrm{P(LH)}}{\Gamma_7} = 2.$$

So even if this laser bandwidth is $\Delta E < E_{\Gamma_7} - E_{\mathrm{LH}}$, it is more likely to produce LH transitions. As we mentioned before in a practical situation, we should be able to prohibit the Γ_7 transition just with these choices.

Now we show that even if we are not able to energetically distinguish the HH and LH transitions the holonomic scheme proposed works as usual. The level scheme for this configuration is shown in Fig. 5. We can excite $E^{\pm}_{\mathrm{HH}}$ excitons or E^0_{LH} exciton. If we have an adiabatic evolution fast enough, the three levels are mixed during the evolution and so, for our scheme, they can be considered degenerate.

The energy gap between HH and LH excitons is of the order of 0.05–0.03 eV [35,42–44], whereas between Γ_7 and HH-LH the gap is about 0.3 eV. Both of these energy gaps are very large compared to the bandwidth of the picosecond and femtosecond pulsed laser, so in practical applications one should be able to separate LH and HH excitons.

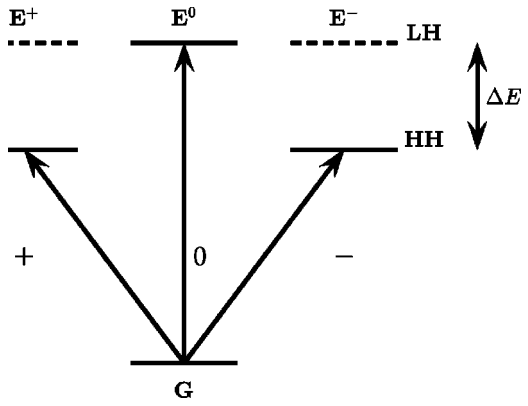

FIG. 5. Level scheme for geometrical gates when is impossible to address only HH or LH.

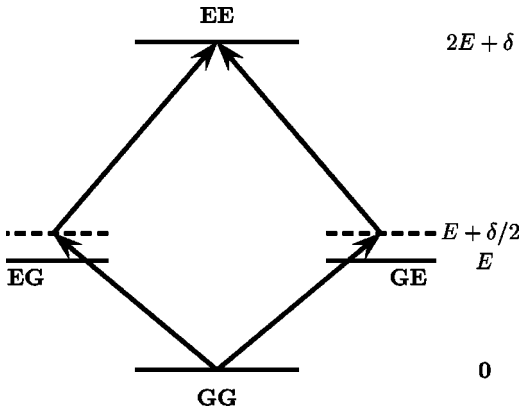

FIG. 6. Level scheme for the two-photon process.

B. Dynamical phase

During the evolution along the adiabatic loop, the state acquires a dynamical phase in addition to the geometrical phase. In the first proposal of adiabatic gates with standard two-level systems, additional work is needed to eliminate this undesidered phase. In Ref. [45] they show how this dynamical phase can be eliminated: we have to run the geometrical gate several times in order to let the dynamical phases cancel each other. The drawback in this method is that we have to iterate several times the adiabatic gate and, because of the adiabatic condition, long time is needed to apply the final geometrical gate.

In this model, if we use LH excitons, the logical and the ancilla states are degenerate and the ground state is never populated during the evolution; so the dynamical phase shift is the same for the two logical qubits and can be neglected.

If we encode logical information in the HH excitons $(\pm)$ and use the LH exciton (0) as ancilla qubit, we have an energy difference ΔE and then a dynamical phase appears. Again, we can neglect it because at the begining (encoding of information) and at the end (reading information) of the evolution, $|E^0\rangle$ state is never populated and then the phase difference does not affect the logical information. Then, in both models, we can avoid problems with the dynamical phase.

V. TWO-QUBIT GATE

For the two-qubit gate, we cannot take directly the Duan-Chirac-Zoller (DCZ) model but we use the biexcitonic shift [13]. In fact if we have two coupled quantum dots, the presence of an exciton in one of them (e.g., in dot b) produces a shift in the energy level of the other (e.g., dot a) from E to $E+\delta/2$.

Let us consider the two dots in the ground state $|GG\rangle$; if we shine them with circular (positive or negative) light at $E+\delta/2$ energy, we should be able to produce two excitons $|EE\rangle$ (see Appendix A). For energy conservation, this is the only possible transition (the absorption of a single photon is at energy E). The detuning allows us to isolate the two-exciton space ($|EE\rangle$) from the single-exciton space ($|EG\rangle$, $|GE\rangle$). The level scheme is shown in Fig. 6.

To show how the two-photon process happens, we solved numerically the Schrödinger equation for a four-level system ($|EE\rangle$, $|EG\rangle$, $|GE\rangle$, $|GG\rangle$). In Fig. 7(a), we show the popu-

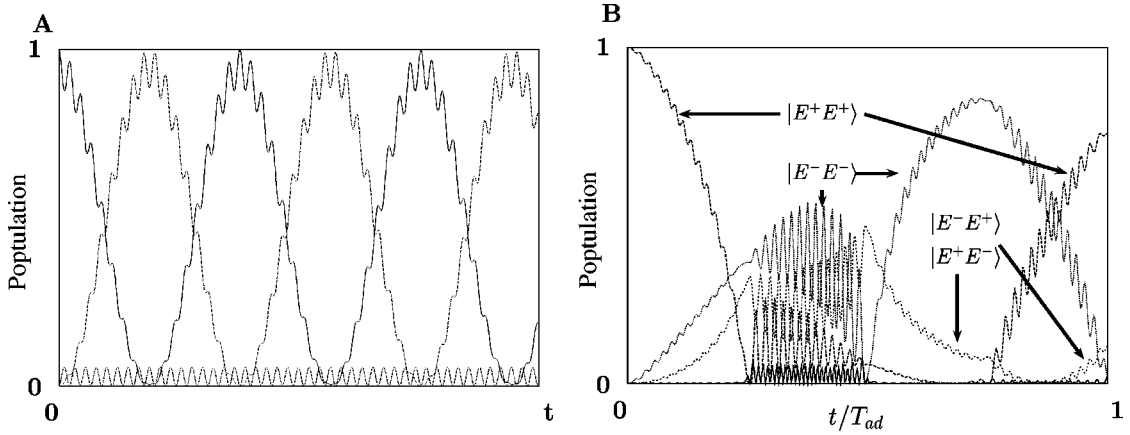

FIG. 7. (a) Production of a biexciton state and isolation of the $|E^i\rangle^{\otimes 2}-|G\rangle^{\otimes 2}$ space. The Rabi oscilation between $|E^i\rangle^{\otimes 2}$ and $|G\rangle^{\otimes 2}$ states are evident and the states $|EG\rangle$ and $|GE\rangle$ are weakly populated. (b) Simulated population evolution for the two-qubit gate. The values of the parameters are $\delta=5$ meV, $|\Omega_{+,-}|=\delta/15$ (for single laser Rabi frequency) , $T_{ad}=0.8$ ns. The gate fidelity $F=|\langle\Psi_{ideal}|\Psi(T_{ad})\rangle|^2=0.9859$.

lation evolution of the states; the Rabi oscillations between $|EE\rangle$ and $|GG\rangle$ are evident and the states $|EG\rangle$, $|GE\rangle$ are weakly populated. In order to fulfill the perturbation condition and clearly show Rabi oscillations we choose $\delta/\Omega = 15$.

We have another degree of freedom in our system: the polarization. Shining the dot with circular or linear polarization, we will obtain $|GG\rangle \rightarrow |E^i E^j\rangle$ $(i,j=+,-,0)$ and can reproduce the scheme with polarized excitons. The general Hamiltonian for the two-photon process is (in interaction representation)

$$H_{int} = -\frac{2\hbar^2}{\delta} \sum_{i,j=+,-,0} (\tilde{\Omega}_i \tilde{\Omega}_j e^{i(\phi_i+\phi_j)} |E^i E^j\rangle\langle GG| + \text{H.c.}). \tag{14}$$

The total two-exciton space has dimension nine but we can restrict to four-dimensional space, turning off the two laser with the same polarization (i.e., $-$ or 0), and because of this situation the scheme is slightly different from the one proposed in the other papers. In Ref. [18], we show how to construct a phase gate; turning on the $+$ and 0 lasers and modulating them to simulate the evolution in gate 1, we were able to obtain the geometrical operator $U_3 = \exp(i\phi |E^+\rangle\langle E^+|^{\otimes 2})$. We can decouple the logical states with negative energy, but we still need four lasers (two with $+$ polarization and two with 0 polarization) to produce a loop in the $|E^+\rangle^{\otimes 2} - |E^0\rangle^{\otimes 2}$ space. The $+$ and 0 lasers must be resonant with the two-exciton transition, but in this scheme we also produce nonlogical states $|E^+E^0\rangle$ and $|E^0E^+\rangle$ since they have the same energy $(\omega_i^1 + \omega_j^1 = 2E + \delta)$. Then we have a bigger dark space with dimension three, and the scheme is not directly repeated. A detailed calculation of the dark states is given in Appendix B.

Now we show how to construct another two-qubit geometrical operator with the same scheme. Since, in general, an adiabatic loop will produce a superposition of *all* the dark states, we change the laser polarization $(0 \rightarrow -)$ so that the system can evolve in the logical space. We note that the space is big enough to produce nontrivial transformation even without the ancilla qubits.

We choose the single-laser Rabi frequencies in order to have $\Omega^{++} = \Omega \sin(\theta/2)$, $\Omega^{--} = \Omega \cos(\theta/2)$, $\Omega^{+-} = \Omega\sqrt{|\sin(\theta/2)\cos(\theta/2)|}$, where $0 \leqslant \theta \leqslant 4\pi$. The dark state are

$$|D_1\rangle = \cos\frac{\theta}{2}|++\rangle - \sin\frac{\theta}{2}|--\rangle,$$

$$|D_2\rangle = \frac{1}{\sqrt{2}}(|+-\rangle - |-+\rangle),$$

$$|D_3\rangle = \sqrt{\frac{|\sin\theta|}{1+|\sin\theta|}}\left(\sin\frac{\theta}{2}|++\rangle + \cos\frac{\theta}{2}|--\rangle\right) - \frac{1}{\sqrt{2(1+|\sin\theta|)}}(|+-\rangle + |-+\rangle). \tag{15}$$

The associated connection is

$$A_\theta = \begin{pmatrix} 0 & 1/2\sqrt{\dfrac{|\sin\theta|}{1+|\sin\theta|}} \\ -1/2\sqrt{\dfrac{|\sin\theta|}{1+|\sin\theta|}} & 0 \end{pmatrix}. \tag{16}$$

Of course, for different values of θ, $[A_\theta, A_{\theta'}] = 0$ and we can calculate the loop integral and then the holonomy. From numerical calculation, we have

$$\alpha = \oint 1/2\sqrt{\frac{|\sin\theta|}{1+|\sin\theta|}}d\theta = \int_0^{4\pi} 1/2\sqrt{\frac{|\sin\theta|}{1+|\sin\theta|}}d\theta = 3.6806$$

and for the holonomic operator,

$$U = e^{i\alpha\sigma_y} = \begin{pmatrix} \cos\alpha & \sin\alpha \\ -\sin\alpha & \cos\alpha \end{pmatrix}. \tag{17}$$

We write explicitly the final state using $|D_1(4\pi)\rangle = |E^+\rangle^{\otimes 2}$ and $|D_2(4\pi)\rangle = 1/\sqrt{2}(|E^+E^-\rangle + |E^-E^+\rangle)$,

$$U|E^+\rangle^{\otimes 2} = \cos\alpha |E^+\rangle^{\otimes 2} - \frac{\sin\alpha}{\sqrt{2}}(|E^+E^-\rangle + |E^-E^+\rangle). \tag{18}$$

This is an entangling gate, and then we have another nontrivial gate.

Now we have to satisfy both the second-order perturbative [from Eq. (14), $\delta/|\Omega_i|^2 \gg 1$] and the adiabatic requirement; this implies that $T_{ad} \gg \delta/|\Omega_i|^2 \gg 1/|\Omega_i|$. Because of the two-photon scheme the operation times for the two-qubit gates are necessarily longer than the ones for the single qubit.

In Fig. 7, we show the numerical simulation obtained by solving the Schrödinger equation. It is difficult to follow the evolution of the states because of the number of the states populated during the evolution and because of their mixing. Moreover, it can be noted that $|GG\rangle$ state never appears in the evolution, $|E^-\rangle^{\otimes 2}$ state is not present at the end of the evolution, and the final state is a superposition of $|E^+\rangle^{\otimes 2}$ and (symmetrically) $|E^+E^-\rangle - |E^-E^+\rangle$ state. In the simulations, we choose $\delta = 5$ meV (as in Ref. [13]) and, for single-laser Rabi frequency, $|\Omega_i| = \delta/15$ (to satisfy the perturbation request); with these parameters, the adiabatic time is $T_{ad} = 0.8$ ns.

VI. CONCLUSIONS

In summary, we have shown that geometrical gates can be implemented in quantum dots with optical control. We use polarized excitons to encode logical information and we have been able to construct a universal set of geometrical quantum gates. The biexcitonic shift due to exciton-exciton dipole coupling is exploited to implement the two-qubit gates. Numerical simulations clearly suggest that one should able to apply several (a few) single-qubit (two-qubit) holo-

nomic gates within the decoherence time.

Even though the fault-tolerance features of this geometrical approach have not been completely clarified so far (see e.g., Ref. [46]), HQC surely provides, on one hand, a sort of an intermediate step towards topological quantum computing and on the other hand, it is a natural arena in which we explore fascinating quantum phenomena.

Finally, we hope that the theoretical investigations presented here will be effective in stimulating novel experimental activity in the field of coherent phenomena in semiconductor nanostructures.

ACKNOWLEDGMENT

Funding by European Union project TOPQIP Project (Contract No. IST-2001-39215) is gratefully aknowledged.

APPENDIX A: TWO-PHOTON PROCESS

Here we show how a two-photon process may occur in our system. Let us consider two coupled quantum dots. The energy-level spacing in this case is different, in fact the presence of an exciton in one of them (e.g., in dot b) produces a shift in the energy level of the other (e.g., dot a) from E to $E+\delta/2$. We have the following Hamiltonian:

$$H_0=(2E+\delta)(|E\rangle\langle E|)^{\otimes 2}+E(|EG\rangle\langle EG|+|GE\rangle\langle GE|). \tag{A1}$$

Using two lasers with frequencies $\omega=(E+\delta/2)$ ($\hbar=1$), the interaction Hamiltonian is [we explicitly take into account the time dependence $\Omega_i=\tilde{\Omega}_i e^{-i\omega t}$ from Eq. (11)]

$$H_{int}=-\hbar\sum_{i=1,2}(\tilde{\Omega}_i e^{-i\omega t}|E_i\rangle\langle G_i|+\tilde{\Omega}_i^* e^{i\omega t}|G_i\rangle\langle E_i|). \tag{A2}$$

The effective Hamiltonian for the process is (the apex 2 indicate that it is a second-order process)

$$H_{int}^{(2)}=-\hbar\tilde{\Omega}e^{-i\tilde{\omega}t}|E\rangle\langle G|^{\otimes 2}+\text{H.c.}, \tag{A3}$$

where $\tilde{\omega}=2\omega$ is the frequency that produces the transition between $|GG\rangle$ and $|EE\rangle$. There are four possible states ($|GG\rangle$, $|EG\rangle$, $|GE\rangle$, $|EE\rangle$); let the initial state be $|GG\rangle$ and we want to know the amplitude coefficient for the $|GG\rangle\rightarrow|EE\rangle$ (Fig. 6). To do this we use the interaction picture,

$$\langle i|e^{iH_0t/\hbar}H_{int}e^{-iH_0t/\hbar}|j\rangle=e^{i(\omega_i-\omega_j)t}e^{\pm i\omega t}\langle i|\tilde{H}_{int}|j\rangle \tag{A4}$$

(the matrix element $\langle i|\tilde{H}_{int}|j\rangle$ is time independent) with the initial conditions $|\psi(0)\rangle=|GG\rangle$ ($|\psi(t)\rangle=\Sigma c_{ij}(t)|ij\rangle$, $i,j=E,G$), $\omega'=\omega_{EE}-\omega_m$, and $\omega''=\omega_m$, with perturbation theory to the second order, we get ($|m\rangle$'s are the intermediate states $|EG\rangle$ and $|GE\rangle$ with energy $E=\hbar\omega_m$)

$$c_{EE}^{(2)}(t)=\left(-\frac{i}{\hbar}\right)^2\sum_m\int_0^t d\tau_1\langle EE|\tilde{H}_{int}|m\rangle e^{i(\omega'-\omega)\tau_1}\times\int_0^{\tau_1}d\tau_2\langle m|\tilde{H}_{int}|GG\rangle e^{i(\omega''-\omega)\tau_2}. \tag{A5}$$

Using $\omega''+\omega'-2\omega=0$, performing the double integration, we get

$$c_{EE}^{(2)}(t)=\left(-\frac{i}{\hbar}\right)^2\sum_m\langle EE|\tilde{H}_{int}|m\rangle\langle m|\tilde{H}_{int}|GG\rangle\frac{1}{i(\omega''-\omega)}\times\left(t-\frac{e^{i(\omega'-\omega)t}-1}{i(\omega'-\omega)}\right). \tag{A6}$$

The term $1-e^{i(\omega'-\omega)t}i(\omega'-\omega)$ oscillates so the leading term is proportional to t

$$c_{EE}^{(2)}(t)\approx\frac{i}{\hbar^2}\sum_m\frac{\langle EE|\tilde{H}_{int}|m\rangle\langle m|\tilde{H}_{int}|GG\rangle}{\omega''-\omega}t. \tag{A7}$$

Now we go back to the second-order Hamiltonian (A3) (two-photon process) and calculate the evolution ($\Delta\omega=\omega_{EE}=2\omega$ and $\Delta\omega-\tilde{\omega}=0$)

$$\begin{aligned}c_{EE}^{(2)}&=-\frac{i}{\hbar}\int_0^t dt_1\langle EE|\tilde{H}_{int}^{(2)}|GG\rangle e^{i(\Delta\omega-\tilde{\omega})t_1}\\&=-\frac{i}{\hbar}\langle EE|\tilde{H}_{int}^{(2)}|GG\rangle\int_0^t dt_1\\&=-\frac{i}{\hbar}(-\hbar\tilde{\Omega})t\\&=i\tilde{\Omega}t.\end{aligned} \tag{A8}$$

The two $c_{EE}^{(2)}$'s are calculated to the same order, so using Eqs. (A6) and (A8),

$$\tilde{\Omega}=\frac{1}{\hbar^2}\sum_m\frac{\langle EE|\tilde{H}_{int}|m\rangle\langle m|\tilde{H}_{int}|GG\rangle}{\omega''-\omega}. \tag{A9}$$

In our system,

$$\begin{aligned}\langle EE|\tilde{H}_{int}|EG\rangle\langle EG|\tilde{H}_{int}|GG\rangle&=\langle EE|\tilde{H}_{int}|GE\rangle\times\langle GE|\tilde{H}_{int}|GG\rangle\\&=\hbar^2\tilde{\Omega}_1\tilde{\Omega}_2\end{aligned} \tag{A10}$$

and we have the Rabi frequency for the two-photon process as function of the single-photon process ($\omega_m''-\omega=\delta/\hbar$).

$$\tilde{\Omega}=\frac{2\hbar\tilde{\Omega}_1\tilde{\Omega}_2}{\delta}. \tag{A11}$$

We take into account the two-exciton production for E^+ and E^0, and choose $\tilde{\Omega}_{1i}=\tilde{\Omega}_i$, $\tilde{\Omega}_{2i}=\tilde{\Omega}_i e^{i\varphi_i}$ with $i=+,0$. The phenomenological Hamiltonian (A3) became

$$H_{int}=-\frac{2\hbar^2}{\delta}\tilde{\Omega}^2 e^{i\varphi}|E\rangle\langle G|^{\otimes 2}+\text{H.c.} \tag{A12}$$

APPENDIX B: HOLONOMIC STRUCTURE OF THE TWO-PHOTON PROCESS

To explicitly calculate the dark state of Hamiltonian (14), we change notation and include the phase in the definition of Rabi frequencies $\Omega^{ij}=\tilde{\Omega}_i\tilde{\Omega}_j e^{i(\phi_i+\phi_j)}$, rewrite the Hamiltonian taking account of production of the same spin excitons ($i=j$), choose the loop in order to have symmetric Rabi frequencies $\Omega^{ij}=\Omega^{ji}$, and we obtain (with $|E^i\rangle=|i\rangle$):

$$H_{int}=-\frac{2\hbar^2}{\delta}(\Omega^{++})^*|++\rangle+(\Omega^{jj})^*|jj\rangle+(\Omega^{+j})^*(|+j\rangle + |j+\rangle)\langle GG|+\text{H.c.}, \tag{B1}$$

where we can take $j=0,-$ to implement different gates since we reduce the dark space and work with just two polarized excitons.

In addition to the decoupled states which do not appear in Eq. B1, we have three dark states ($\Omega^2=|\Omega^{++}|^2+|\Omega^{jj}|^2$):

$$|D_1\rangle=\frac{(\Omega^{jj})^*|++\rangle-(\Omega^{++})^*|jj\rangle}{\Omega},$$

$$|D_2\rangle=\frac{1}{\sqrt{2}}(|+j\rangle-|j+\rangle),$$

$$|D_3\rangle=\frac{1}{\Omega\sqrt{|\Omega^{ij}|^2+\Omega^2/2}}[(\Omega^{ij})^*(\Omega^{++}|++\rangle+\Omega^{jj}|jj\rangle) - \frac{\Omega^2}{2}(|+j\rangle+|j+\rangle)]. \tag{B2}$$

Now we can explicitly calculate some connection for particular loops. we choose $j=0$ for the laser Rabi frequencies $\Omega_i^+=\sqrt{\Omega\sin(\theta/2)}\exp(i\varphi/2)$, $\Omega_i^0=\sqrt{\Omega\cos(\theta/2)}$ ($i=1,2$ is the dot index), and we use a loop in the θ and ϕ plane similar to the one in Fig. 2 ($0\leqslant\theta\leqslant\pi$ and $0\leqslant\phi\leqslant\pi/2$); then we have for the effective Rabi frequencies

$$\Omega^{++}=\Omega\sin\frac{\theta}{2}e^{i\varphi},$$

$$\Omega^{00}=\Omega\cos\frac{\theta}{2},$$

$$\Omega^{+0}=\Omega\sqrt{\sin\frac{\theta}{2}\cos\frac{\theta}{2}}\exp(i\varphi/2). \tag{B3}$$

The dark states in Eq. (B2) explicitly take the form

$$|D_1\rangle=\cos\frac{\theta}{2}|++\rangle-\sin\frac{\theta}{2}e^{-i\varphi}||00\rangle,$$

$$|D_2\rangle=\frac{1}{\sqrt{2}}(|+0\rangle-|0+\rangle),$$

$$|D_3\rangle=\sqrt{\frac{\sin\theta}{1+\sin\theta}}\left(\sin\frac{\theta}{2}e^{i\varphi/2}|++\rangle+\cos\frac{\theta}{2}e^{-i\varphi/2}|00\rangle\right) - \frac{1}{\sqrt{2(1+\sin\theta)}}(|+0\rangle+|0+\rangle). \tag{B4}$$

The connection associated is

$$A_\theta=\begin{pmatrix} 0 & 1/2\sqrt{\frac{\sin\theta}{2+\sin\theta}}e^{i\varphi/2} \\ -1/2\sqrt{\frac{\sin\theta}{1+\sin\theta}}e^{-i\varphi/2} & 0 \end{pmatrix}, \tag{B5}$$

$$A_\varphi=\begin{pmatrix} -i\sin^2\frac{\theta}{2} & i/2\sqrt{\frac{\sin\theta}{2+\sin\theta}}\sin\theta\, e^{i\varphi/2} \\ i/2\sqrt{\frac{\sin\theta}{1+\sin\theta}}\sin\theta e^{-i\varphi/2} & i/2\frac{\sin\theta}{1+\sin\theta} \end{pmatrix}. \tag{B6}$$

The holonomic operator cannot be analytically calculated because the connections do not commute. Then we calculated it with computer simulations by discretization of the loop in the parameter space.

[1] P.W. Shor, in *Proceeding of 35th Annual Symposium on Foundation of Computer Science*, edited by S. Goldwasser (IEEE Computer Society Press, Los Alamitos, CA, 1994).

[2] P.W. Shor, Phys. Rev. A **52**, 2493 (1995); A.M. Steane, Phys. Rev. Lett. **77**, 793 (1996); E. Knill and R. Laflamme, Phys. Rev. A **55**, 900 (1997), and references therein.

[3] P. Zanardi and M. Rasetti, Phys. Rev. Lett. **79**, 3306 (1997).

[4] L. Viola, E. Knill, and S. Lloyd, Phys. Rev. Lett. **82**, 2417 (1999), and references therein.

[5] P. Zanardi, Phys. Lett. A **258**, 77 (1999).

[6] I.L. Chuang *et al.*, Phys. Rev. Lett. **80**, 3408 (1998).

[7] J.I. Cirac and P. Zoller, Phys. Rev. Lett. **74**, 4091 (1995).

[8] A. Sørensen and K. Mølmer, Phys. Rev. Lett. **82**, 1971 (1999).

[9] K. Mølmer and A. Sørensen, Phys. Rev. Lett. **82**, 1935 (1999).

[10] J.I. Cirac and P. Zoller, Nature (London) **404**, 579 (2000).

[11] D.P. DiVincenzo and D. Loss, Phys. Rev. A **57**, 120 (1998).

[12] P. Zanardi and F. Rossi, Phys. Rev. Lett. **81**, 4752 (1998).

[13] E. Biolatti *et al.*, Phys. Rev. Lett. **85**, 5647 (2000); E. Biolatti

et al., Phys. Rev. B **65**, 07536 (2002).
[14] A. Kitaev, e-print quant-ph/9707021.
[15] M.H. Freedman, A. Kitaev, and W. Zhenghan, Commun. Math. Phys. **227**, 587 (2002).
[16] P. Zanardi and M. Rasetti, Phys. Lett. A **264**, 94 (1999).
[17] J. Pachos, P. Zanardi, and M. Rasetti, Phys. Rev. A **61**, 010305(R) (2000).
[18] Solinas *et al.*, e-print quant-ph/0207019.
[19] M.V. Berry, Proc. R. Soc. London, Ser. A **392**, 45 (1984).
[20] F. Wilczek and A. Zee, Phys. Rev. Lett. **52**, 2111 (1984).
[21] J.A. Jones *et al.*, Nature (London) **403**, 869 (2000).
[22] G. Falci *et al.*, Nature (London) **407**, 355 (2000).
[23] J. Preskill, in *Introduction to Quantum Computation and Information*, edited by H.-K. Lo, S. Poposcu, and T. Spiller (World Scientific, Singapore, 1999).
[24] D. Ellinas and J. Pachos, Phys. Rev. A **64**, 022310 (2001).
[25] W. Xiang-Bin and M. Keiji, Phys. Rev. Lett. **87**, 097901 (2001); see also, *ibid.* **88**, 179901(E) (2002).
[26] X.-Q. Li *et al.*, Phys. Rev. A **66**, 042320 (2002).
[27] S.L. Zhu and Z.D. Wang, Phys. Rev. Lett. **89**, 097902 (2002).
[28] P. Solinas *et al.*, e-print quant-ph/0301089.
[29] R.G. Unanyan, B.W. Shore, and K. Bergmann, Phys. Rev. A **59**, 2910 (1999).
[30] L.-M. Duan, J.I. Cirac, and P. Zoller, Science **292**, 1695 (2001).
[31] L. Faoro, J. Siewert, and R. Fazio, Phys. Rev. Lett. **90**, 028301 (2003).
[32] I. Fuentes-Guridi *et al.*, Phys. Rev. A **66**, 022102 (2002).
[33] A. Recati *et al.*, Phys. Rev. A **66**, 032309 (2002).
[34] R.T. Collins *et al.*, Phys. Rev. B **36**, 1531 (1987).
[35] J.-Y. Marzin *et al.*, Phys. Rev. B **31**, 8298 (1985).
[36] G. Bastard, *Wave Mechanics Applied to Semiconductor Heterestructures* (Les editions de physique, Paris, 1982).
[37] S.S. Schimtt-Rink *et al.*, Phys. Rev. B **46**, 10 460 (1992).
[38] M. Bayer *et al.*, Science **291**, 451 (2001).
[39] J. Shah, *Ultrafast Spectroscopy of Semiconductors and Semiconductor Nanostructures* (Springer, Berlin, 1996).
[40] P. Borri *et al.*, Phys. Rev. Lett. **87**, 157401 (2001).
[41] A.O. Niskanen, M. Nakahara, and M.M. Salomaa, Phys. Rev. A **67**, 012319 (2003).
[42] R.C. Miller *et al.*, Phys. Rev. B **22**, 863 (1980).
[43] R.C. Miller *et al.*, Phys. Rev. B **24**, 1134 (1981).
[44] Y. Matsumoto, *et al.*, Phys. Rev. B **32**, 4275 (1985).
[45] A. Ekert *et al.*, J. Mod. Opt. **47**, 2501 (2000).
[46] A. Nazir, T.P. Spiller, and W.J. Munro, Phys. Rev. A **65**, 042303 (2002); A. Blais, A.-M.S. Tremblay, A. Blais, and A.-M.S. Tremblay, *ibid.* **67**, 012306 (2003).